

$f(\alpha)$ Multifractal spectrum at strong and weak disorder

E. Cuevas*

Departamento de Física, Universidad de Murcia, E-30071 Murcia, Spain.

(Dated: October 29, 2018)

The system size dependence of the multifractal spectrum $f(\alpha)$ and its singularity strength α is investigated numerically. We focus on one-dimensional (1D) and 2D disordered systems with long-range random hopping amplitudes in both the strong and the weak disorder regime. At the macroscopic limit, it is shown that $f(\alpha)$ is parabolic in the weak disorder regime. In the case of strong disorder, on the other hand, $f(\alpha)$ strongly deviates from parabolicity. Within our numerical uncertainties it has been found that all corrections to the parabolic form vanish at some finite value of the coupling strength.

PACS numbers: 71.30.+h, 05.45.Df, 72.15.Rn, 73.20.Jc

I. INTRODUCTION

In recent years, it has become clear that the eigenfunctions of noninteracting disordered systems at the critical point of a metal-insulator transition (MIT) have multifractal scaling properties. Hence, multifractal analysis has become a standard tool for treating the strong wave-function fluctuations which arise near criticality.¹ One way to characterize wave-function statistics is through the corresponding multifractal $f(\alpha)$ spectrum. This spectrum of the local density is universal at the critical point, and the exponents such as α_0 , which describes the scaling behavior of the typical local electron density, are suitable for describing the phase transition.² Finding the true $f(\alpha)$ curve is essential in order to fully understand MITs.

MITs depend on the dimensionality and symmetries of the system and can occur in both the strong disorder and the weak disorder regime (strong-coupling or weak-coupling regime, respectively, in the language of field theory). Each regime is characterized by the corresponding coupling strength that depends on the ratio between diagonal disorder and the off-diagonal transition matrix elements of the Hamiltonian.³ We wish to point out that most of the already published analytical results concerning the $f(\alpha)$ spectrum, which we summarize in the next paragraphs, have been obtained in the weak disorder limit (weak-coupling approach).

Using the renormalization group in $d = 2 + \epsilon$ dimensions ($\epsilon = \alpha_0 - d \ll 1$), it was found⁴ that the singularity spectrum is parabolic,

$$f(\alpha) = d - \frac{(\alpha - \alpha_0)^2}{4(\alpha_0 - d)}, \quad (1)$$

up to $O(\epsilon^2)$. This equation was justified for the case of unbroken time-reversal symmetry (orthogonal universality class) in the weak-coupling limit.

Recently, in Ref. 5 it was found that a parabolic spectrum (PS) is fulfilled for the critical wave function of a two-dimensional (2D) Dirac fermion in a random vector potential (chiral universality class). These results were obtained by mapping the problem to a Gaussian field theory in an ultrametric space (a Cayley tree). For a deep

understanding of the origin of the multifractal behavior in this model, see also Ref. 6.

The field-theoretical approaches in the context of the integer quantum Hall transition (unitary universality class) has been addressed more recently. Based on the application of conformal field theory to the critical point of a 2D Euclidean field theory, Bhaseen *et al.*⁷ conjectured that the singularity spectrum is exactly parabolic at the plateau transitions. Using the same general principles of conformal field theory,^{8,9} a PS was conjectured for a closely related quantity, the two-point conductance.

Given the present status of this problem, it would be highly desirable to check (i) whether the PS is fulfilled at weak disorder strength and (ii) whether or not the PS holds in the strong disorder regime, where it is known that all realistic MITs, such as the conventional Anderson transition in 3D, take place. Unfortunately, because of the absence of a small parameter, no quantitative predictions for the critical properties and, in particular, for the $f(\alpha)$ spectrum have been made in the strong-coupling regime. In the absence of such predictions, the problem must be addressed using numerical calculations. That is why we are interested in exploring the role of the disorder strength on the $f(\alpha)$ spectrum. Specifically, we want to analyze how the singularity spectrum evolves in the face of increasing coupling strength, i.e., when the transition shifts from the weak disorder regime to the strong disorder regime.

This paper is organized as follows. In Sec. I, we introduce the model and the methods used for the calculations. The results for the multifractal spectrum in 1D and 2D are shown in Secs. II A and II B, respectively. Finally, the conclusions are presented in Sec. III.

II. MODEL AND METHODS

For computation of the multifractal spectrum, we use the standard box-counting procedure,² first dividing the system of L^d sites into $N_l = (L/l)^d$ boxes of linear size l and determining the box probability of the wave function in the i box by $\mu_i(l) = \sum_n |\psi_{kn}|^2$, where the summation is restricted to sites within that box and ψ_{kn} denotes the

amplitude of an eigenstate with energy E_k at site n . The normalized q th moments of this probability $\mu_i(q, l) = \mu_i^q(l) / \sum_{j=1}^{N_l} \mu_j^q(l)$ constitute a measure. From this, the Lipschitz-Hölder exponent or singularity strength can be obtained,¹⁰

$$\alpha_q(L) = \lim_{\delta \rightarrow 0} \frac{\sum_{i=1}^{N_l} \mu_i(q, l) \ln \mu_i(1, l)}{\ln \delta}, \quad (2)$$

as well as the corresponding fractal dimension

$$f(\alpha_q(L)) = \lim_{\delta \rightarrow 0} \frac{\sum_{i=1}^{N_l} \mu_i(q, l) \ln \mu_i(q, l)}{\ln \delta}, \quad (3)$$

which yields the characteristic singularity spectrum $f(\alpha)$ in a parametric representation. In Eqs. (2) and (3), $\delta = l/L$ denotes the ratio of the box sizes and the system size. If the q th moments of the measure counted in all boxes are proportional to a power τ_q of the box size, $\langle \sum_{i=1}^{N_l} \mu_i^q(l) \rangle \propto l^{-\tau_q}$, multifractal behavior may be derived. The $f(\alpha)$ spectrum and the mass exponent τ_q are related by a symmetric Legendre transformation, $f(\alpha) = \alpha q - \tau_q$, with $\alpha = d\tau_q/dq$ and $q = df(\alpha)/d\alpha$. From Eq. (1), one can easily obtain

$$\alpha_0 - d = d - \alpha_1. \quad (4)$$

In what follows, we will first use this relation to check whether or not the PS is valid in each regime studied. First, $\alpha_q(L)$ and $f(\alpha_q(L))$ were calculated for different system sizes and then extrapolated to the macroscopic limit $\alpha_q = \lim_{L \rightarrow \infty} \alpha_q(L)$ and $f(\alpha_q) = \lim_{L \rightarrow \infty} f(\alpha_q(L))$. We wish to clarify that the calculation of $\alpha_q(L)$ and $f(\alpha_q(L))$ is suitable only if the conditions²

$$a \ll l < L \ll \xi \quad (5)$$

are satisfied, where ξ is the localization or correlation length and a is the lattice spacing (or any microscopic length scale of the system, such as the cyclotron radius).

Usually, the disorder-induced MIT is investigated for Hamiltonians with short-range, off-diagonal matrix elements (e.g., the canonical Anderson model). Another class of Hamiltonian exhibiting an MIT in arbitrary dimension d is formed by those that include long-range hopping terms. The effect of long-range hopping on localization was originally considered by Anderson¹¹ for randomly distributed impurities in d dimensions with the $V(\mathbf{r} - \mathbf{r}') \sim |\mathbf{r} - \mathbf{r}'|^{-\beta}$ hopping interaction. It is known^{11,12} that all states are extended for $\beta \leq d$, whereas for $\beta > d$, the states are localized. Thus, one can study the MIT by varying the exponent β at fixed disorder strength. At the transition line $\beta = d$, a real-space renormalization group can be constructed for the distribution of couplings.^{12,13} These models are most convenient for studying critical properties because the exact critical point is known ($\beta = d$) and they allow us to treat the 1D and 2D cases, thus reaching larger system sizes

and reducing the numerical effort. Here, we will concentrate on the 1D and 2D versions of these models with orthogonal symmetry. In our calculations, we consider a small energy window, containing about 8% of the states around the center of the spectral band. The number of random realizations is such that the number of critical states included for each L is roughly 4×10^5 , while in order to reduce the edge effects, periodic boundary conditions in all directions are included. Using methods based on level statistics, we checked that the normalized nearest level variances¹⁴ are indeed scale invariant at each critical point studied.

A. 1D system

First, we concentrate on the intensively studied power-law random banded matrix model (PRBM).^{15,16,17,18,19} The corresponding Hamiltonian that describes a disordered 1D sample with random long-range hopping is represented by real symmetric matrices, whose entries are randomly drawn from a normal distribution with zero mean, $\langle \mathcal{H}_{ij} \rangle = 0$, and a variance which depends on the distance between lattice sites,

$$\langle |\mathcal{H}_{ij}|^2 \rangle = \frac{1}{1 + (|i - j|/b)^2} \times \begin{cases} \frac{1}{2}, & i \neq j \\ 1, & i = j. \end{cases} \quad (6)$$

The model describes a whole family of critical theories parametrized by $0 < b < \infty$, which determines the critical dimensionless conductance in the same way as the dimensionality labels the different Anderson transitions. In the two limiting cases $b \gg 1$ and $b \ll 1$, which correspond to the weak and the strong disorder limits, respectively, some critical properties have been derived analytically.^{15,16,20,21,22} The system size ranges between $L = 40$ and $L = 1800$, and $0.03 \leq b \leq 30$. We restrict ourselves to values of $q \geq 0$, which correspond to $\alpha \leq \alpha_0$.

Using the exact eigenstates of Eq. (6) from numerical diagonalizations, we obtained the size dependence of the scaling exponents $\alpha_q(L)$ and $f(\alpha_q(L))$ at the critical point of the finite system. In order to extrapolate to macroscopic systems, we propose a finite-size correction to $\alpha_q(L) = \alpha_q + a_q L^{-y_q}$, where the irrelevant exponent $y_q > 0$. For all values of q , we found that the exponent y_q hardly differs from unity. The same behavior is found for $f(\alpha_q(L))$. Thus, we can write

$$\alpha_q(L) = \alpha_q + a_q/L, \quad f(\alpha_q(L)) = f(\alpha_q) + b_q/L, \quad (7)$$

with α_q , a_q , $f(\alpha_q)$, and b_q being adjustable parameters. As we will see below, our numerical data strongly support this behavior.

As a first step, for each value of q , we evaluate the numerators on the right-hand sides of Eqs. (2) and (3), respectively, for decreasing box sizes, and we calculate $\alpha_q(L)$ and $f(\alpha_q(L))$ from the slopes of the graphs of the numerators versus $\ln \delta$. In order to satisfy the inequalities of Eq. (5), we take δ to be in the interval

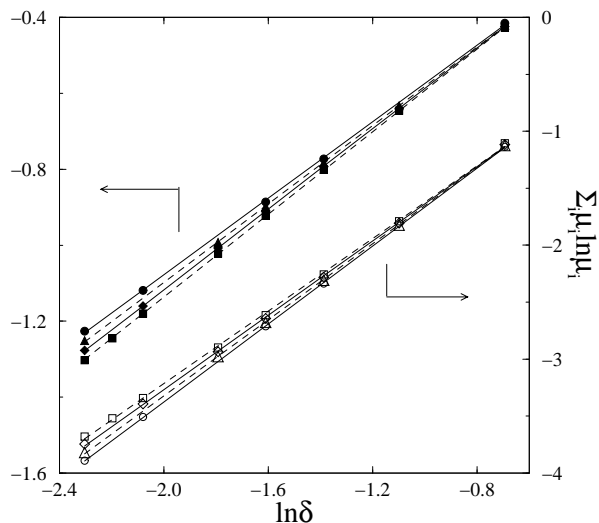


FIG. 1: $\sum_i \mu_i(q, l) \ln \mu_i(1, l)$ as a function of $\ln \delta$ for $q = 0$ (open symbols, right axis) and $q = 1$ (solid symbols, left axis) and different system sizes: $L = 40$ (circles), 60 (triangles), 120 (diamonds), and 1800 (squares). The straight lines whose slopes correspond to the values of $\alpha_0(L)$ and $\alpha_1(L)$ are linear fits to Eq. (2).

(0.1, 0.5). Figure 1 provides an example of the linear fit to $\sum_i \mu_i(q, l) \ln \mu_i(1, l)$ versus $\ln \delta$ for two values of q , $q = 0$ (open symbols, right axis) and $q = 1$ (solid symbols, left axis), and different system sizes: $L = 40$ (circles), 60 (triangles), 120 (diamonds), and 1800 (squares). Clearly, there is no ambiguity in the determination of the slopes that correspond to the values of $\alpha_0(L)$ and $\alpha_1(L)$. These slopes, which are summarized in Fig. 2, have been obtained for $b = 0.3$.

In Fig. 2, we represent the finite-size corrections for the scaling exponents α_0 (circles) and α_1 (squares) for the 1D disordered system described by Eq. (6) in the strong-coupling regime ($b = 0.3$). The straight lines are linear fits to Eq. (7) and intercept the vertical axis at 0.590 and 0.455, respectively. These results clearly demonstrate that Eq. (4) is not fulfilled at all, indicating that the PS is no longer valid in this case. This is not surprising since the parameter found ($\epsilon = 0.590$), is not small, and the ϵ expansion (1) can only be justified parametrically for $\epsilon \ll 1$. We have found that if b is reduced, the intercept points shift to higher values and their separation increases.

The inset of Fig. 2 shows the same L dependence for the case of weak coupling ($b = 10$). Unlike in the strong-coupling regime, both lines intercept the y axis practically at the same values, of 0.0194 and 0.0193, respectively. This suggests that $f(\alpha)$ is parabolic, in agreement with Eq. (1). In this case, $\epsilon = 0.0194 \ll 1$, as expected. Very recently, results similar to those in the inset were obtained for the Chalker-Coddington model, although in this case a different method²³ was used to evaluate $\alpha_q(L)$.

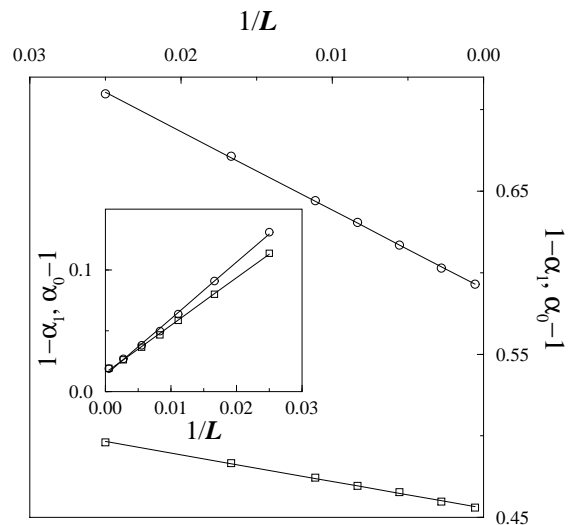


FIG. 2: The L dependence of the scaling exponents α_0 (circles) and α_1 (squares) for the 1D disordered system in the strong-coupling regime ($b = 0.3$). The straight lines are linear fits to Eq. (7). The inset shows the same dependence for the case of weak coupling ($b = 10$).

In this calculation, the parameter found was $\epsilon = 0.26$.

The extrapolated results of the whole $f(\alpha)$ curve in the strong-coupling regime $b = 0.1$ are depicted in Fig. 3 (solid circles). The implicit parameter q ranges from 0 to 1, in steps of 0.1. Note that Eq. (1) is assumed to be valid least up to $|q| \leq 1$.² The PS with $\alpha_0 = 2.228$ is shown for comparison (solid line). The difference between both results is noteworthy. Based on a resonance approximation, the following formula was derived in Ref. 16 for $f(\alpha)$ in the regime $b \ll 1$ for values of $q > \frac{1}{2}$,

$$f(\alpha) = 2bF(\alpha/2b), \quad (8)$$

where $F(A)$ is the Legendre transform of the function $\Gamma(2q-1)/2^{2q-3}\Gamma(q)\Gamma(q-1)$. The result of Eq. (8) for $b = 0.1$ is represented by a dot-dashed line. At $q = \frac{1}{2}$, the mass exponent τ_q diverges, while for smaller values of q , this approximation completely breaks down. Note that $f(\alpha)$ properly interpolates between the parabola and Eq. (8). For the smallest values of q near the maximum, $f(\alpha)$ is very close to the PS, and as q increases, $f(\alpha)$ separates from this curve with a regular tendency until it reaches the resonance prediction for the larger values of q as shown. We have found that as b decreases, the deviations with respect to PS are larger, and as b increases, these deviations diminish. For values of b well inside the weak-coupling domain (see inset), the deviations are practically unobservable. The inset of Fig. 3 shows the same $f(\alpha)$ spectrum for the weak coupling regime ($b = 10$). The perfect agreement between the obtained results (solid circles) and the PS, Eq. (1), with $\alpha_0 = 1.0194$ is evident. Similar results were obtained in

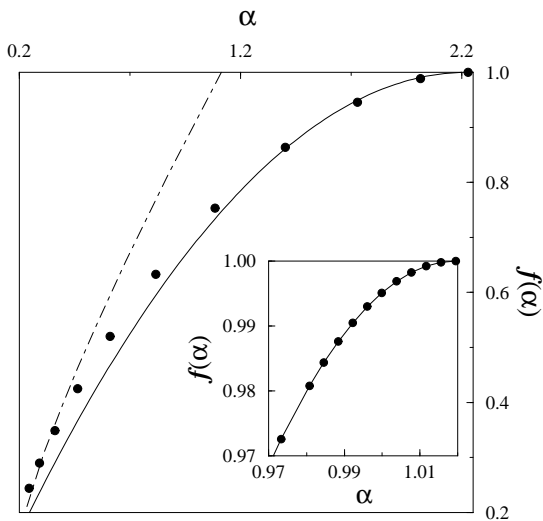


FIG. 3: The $f(\alpha)$ spectrum (solid circles) for the 1D disordered system in the strong-coupling regime ($b = 0.1$). The implicit parameter q ranges from 0 to 1. The PS with $\alpha_0 = 2.228$ is shown for comparison (solid line). The dot-dashed line corresponds to Eq. (8) for $q > 1/2$. The inset shows the same spectrum in the case of weak-coupling ($b = 10$) together with the PS with $\alpha_0 = 1.0194$ (solid line).

Ref. 16 for this regime. We can thus conclude, as we previously stated, that the PS is correct in this case.

B. 2D system

We have also calculated the $f(\alpha)$ spectrum in the experimentally more important case $d = 2$. Unlike the 1D PRBM model, until now, it has not been possible to solve the 2D disordered models with long-range transfer terms analytically. We consider noninteracting electrons on a 2D square lattice with random on-site potentials ε_i and random transfer terms $V_{ij} = V\varepsilon_{ij}/|\mathbf{r}_i - \mathbf{r}_j|^2$, whose Hamiltonian reads

$$\mathcal{H} = \sum_i \varepsilon_i |\mathbf{r}_i\rangle\langle\mathbf{r}_i| + \sum_{i \neq j} V_{ij} |\mathbf{r}_i\rangle\langle\mathbf{r}_j|, \quad (9)$$

where the vectors \mathbf{r}_i label the sites of the lattice, and $\{\varepsilon_i\}$ and $\{\varepsilon_{ij}\}$ are two sets of uncorrelated random numbers uniformly distributed within the interval $(-W/2, W/2)$, and $(-S/2, S/2)$, respectively. $V = 1$ defines the energy scale and S/V is taken to be equal to 1 in all regimes. Each regime is characterized by the coupling strength $\lambda = W/S$ and we take $0.4 \leq W/V \leq 30$. The system sizes used are $L = 24, 36, 56, 72$, and 96 . The critical properties of this model in the strong disorder regime have recently been investigated numerically.²⁴ A closely related model in $d = 1 - 3$ was also considered in Ref. 25 for strong disorder.

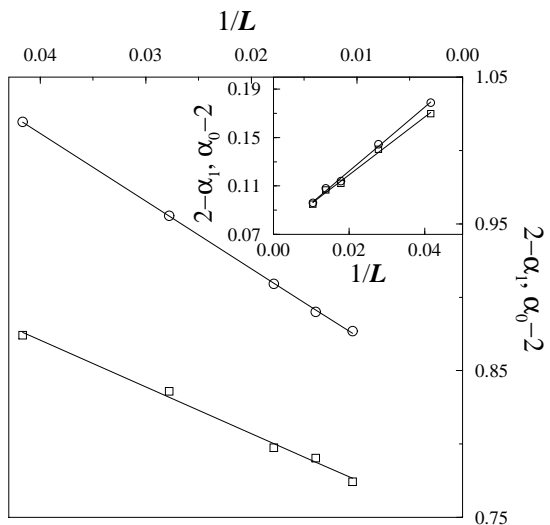


FIG. 4: As for Fig. 2, for the 2D disordered system in the strong-coupling regime ($\lambda = 6$). The results of the inset correspond to the same system in the weak-coupling regime ($\lambda = 0.4$).

In Fig. 4, we show the same size corrections as in Fig. 2 for the 2D disordered system in the strong-coupling regime ($\lambda = 6$). The fitted straight lines intercept the vertical axis at 0.827 and 0.743. The corresponding results for the case of weak coupling ($\lambda = 0.4$) are reported in the inset. As in the 1D system, we obtained a L^{-1} behavior for these corrections in both regimes. All the comments made with respect to the 1D system are equally valid in this case. Hence, we arrive at the same conclusions for the 2D case, i.e., the PS is valid in the weak disorder regime whereas the strong disorder case strongly deviates from this behavior.

Figure 5 shows the same extrapolated values of the $f(\alpha)$ spectrum as in Fig. 3 for the 2D disordered system in the strong disorder regime ($\lambda = 30$). The PS with $\alpha_0 = 4.3673$ is shown for comparison (solid line). As in the 1D case, the difference between both results is notable. As there are no analytical predictions for this regime, we are not able to justify the sign of the deviations in this case. The inset shows the same $f(\alpha)$ spectrum (solid circles) for the weak-coupling regime ($\lambda = 0.4$) together with the PS (solid line) with $\alpha_0 = 2.0692$.

We now define in a simple way the extent to which the spectra deviate from parabolicity. We consider the distance between the two intercept points in Figs. 2 and 4, $\Delta_{\alpha d} = \alpha_0 + \alpha_1 - 2d$, as a measure of departure from the parabolic shape. This clearly distinguishes a parabolic spectrum from a nonparabolic one. In the following, we will use the notations $t_1 = 1/b$ and $t_2 = \lambda$ for the coupling constant of the 1D and 2D models, respectively. In Fig. 6, we represent the dependence with the coupling constant t_d of the parameter $\Delta_{\alpha d}$ for 1D (squares) and 2D (circles) disordered systems. This parameter will

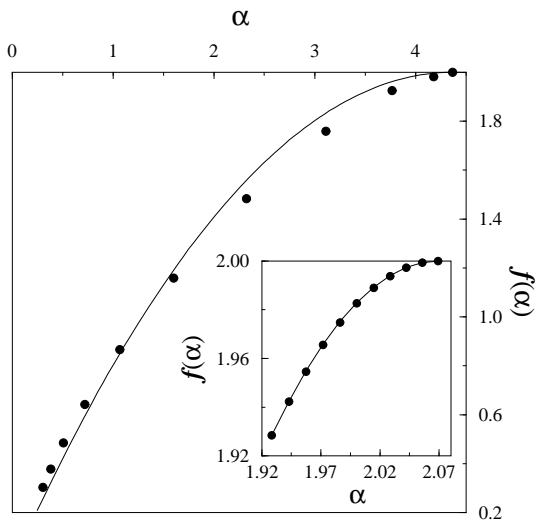


FIG. 5: Same as Fig. 3, for the 2D disordered system in the strong-coupling regime ($\lambda = 30$). The PS with $\alpha_0 = 4.3673$ is shown for comparison (solid line). The inset shows the same spectrum in the case of weak coupling ($\lambda = 0.4$) together with the PS with $\alpha_0 = 2.0692$ (solid line).

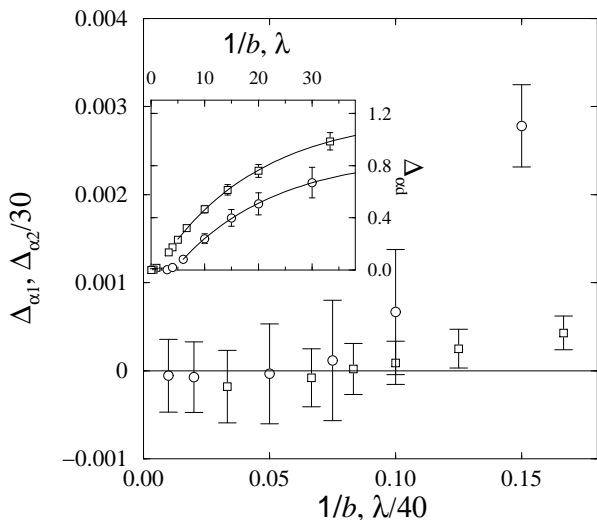


FIG. 6: The small coupling constant dependence of the parameter $\Delta_{\alpha d}$ for the 1D (squares) and 2D (circles) disordered systems. The inset shows the same dependence in the whole range of b and λ studied; solid lines are fits to Eq. (10).

tend to a well-defined finite value in the limit $t_d \rightarrow \infty$. The small t_d -dependent behavior of $\Delta_{\alpha d}$, corresponding to the weak-coupling regime, is shown in the main panel of Fig. 6, in which one can clearly appreciate that below a given value of t_d ($t_1 \approx 0.1$ for the 1D system and $t_2 \approx 4$ for the 2D case), $\Delta_{\alpha d} = 0$ within the error bars. This result strongly suggests that all corrections to parabolicity vanish at a *finite* value of the coupling constant, in

contrast to what might be expected naively.

In order to predict the large t_d asymptotic values of $\Delta_{\alpha d}$ from the inset of Fig. 6, a curve of the form $\Delta_{\alpha d} = \Delta_0 - G_{A,B}(t_d)$ was fitted to the data points in this graph, where Δ_0 , A , and B are three positive fitting parameters, and $G_{A,B}(t_d)$ is a function which goes to zero as $t_d \rightarrow \infty$. Note that this fit was performed only over the larger values of t_d where convergence was evident. Various forms for $G_{A,B}(t_d)$ were chosen and tested on the data plots. These included exponential, inverse logarithmic, and power-law decay with t_d . The testing involved performing a three-parameters fit on the $\Delta_{\alpha d}$ versus t_d data plots using the standard Levenberg-Marquardt method for nonlinear fits. The form of $G_{A,B}(t_d)$ eventually chosen was the exponential law. The reason for choosing the above form of $G_{A,B}(t_d)$ with preference to the alternative forms was simply that the inverse logarithmic and the power laws do not fit our data properly. Thus, the small and large t_d -dependent behavior of $\Delta_{\alpha d}$ can be described by

$$\Delta_{\alpha d} = \begin{cases} 0 & , t_1 \lesssim 0.1, t_2 \lesssim 4 \\ \Delta_0 - Ae^{-Bt_d} & , t_d \gg 1. \end{cases} \quad (10)$$

The solid lines in the inset of Fig. 6 are fits to Eq. (10) with parameters $\Delta_0 = 1.19 \pm 0.02$, $A = 1.250 \pm 0.013$, and $B = 0.054 \pm 0.002$ for the 1D system, and $\Delta_0 = 0.88 \pm 0.02$, $A = 1.110 \pm 0.013$, and $B = 0.055 \pm 0.002$ for the 2D case.

Very recently, Potempa and Schweitzer²⁴ reported the $f(\alpha)$ spectrum for a critical wave function of a finite sample in 2D of linear size $L = 150$ for $\lambda = 6$. For this value of λ , we found $\Delta_{\alpha 2} = 0.084$, indicating that we are very close to the regime where deviations are practically unobservable. These authors found deviations (downwards) from PS mainly for the largest negative q values. We believe that these deviations are due to the use of the finite-size value of α_0 . If the extrapolated value of $\alpha_0 = 2.827$ is used instead, the agreement with the PS is fairly good.

Before concluding, we must admit that experiments to measure α_0 or related multifractal exponents have not been carried out. However, the statistical properties of wave functions are close related to the conductance statistics. As was demonstrated in Ref. 9, multifractality can show up in transport experiments. Specifically, the q th moments of the two-point conductance exhibit multifractal statistics. The connection between the PS for the conductance and Eq. (1) is through the relation $X_t = 2(\alpha_0 - d)$, where X_t is the power-law exponent of the typical conductance. In this way, our results could be checked in experiments with random systems using samples with varying disorder.

III. CONCLUSIONS

In this paper, we have calculated the multifractal scaling exponents of the wave functions for 1D and 2D disordered systems with long-range transfer terms at criti-

cality. The leading finite-size corrections to α and $f(\alpha)$ decay algebraically with exponents equal to -1 . In the limit $L \rightarrow \infty$, we have demonstrate that according to theoretical predictions, the $f(\alpha)$ spectrum is parabolic in the weak disorder regime. Our calculations strongly suggest that the parabolic spectrum completely breaks down for large values of the disorder strength, and more importantly, that all corrections to the parabolic shape vanish (within our numerical uncertainties) at a finite value of the coupling constant.

The question arises as to whether these results are applicable to other quantum systems, particularly in the 3D Anderson transition that occurs in the strong disorder domain, and whose similarity with the PRBM model at $b = 0.3$ has been demonstrated for several critical

magnitudes.¹⁸ Another interesting question is whether the deviations studied here also have signatures in other properties, such as spectral statistics or generalized dimensions. Finally, how the present 2D model can be studied, using 2D conformal field theory or locator expansion instead of the resonance pair approximation, remains to be resolved.

Acknowledgments

The author thanks the Spanish DGESIC for financial support through Project No. BFM2000-1059.

-
- * Electronic address: ecr@um.es;
URL: <http://bohr.fcu.um.es/miembros/ecr/>
- ¹ V.I. Fal'ko and K.B. Efetov, Europhys. Lett. **32**, 627 (1995); Phys. Rev. B **52**, 17413 (1995).
 - ² M. Janssen, Int. J. Mod. Phys. B **8**, 943 (1994); B. Huckestein, Rev. Mod. Phys. **67**, 357 (1995).
 - ³ K.B. Efetov, Adv. Phys. **32**, 53 (1983).
 - ⁴ C. Castellani and L. Peliti, J. Phys. A **19**, L429 (1986); F. Wegner, Nucl. Phys. B **280**, 210 (1987).
 - ⁵ C.C. Chamon, C. Mudry, and X.-G. Wen, Phys. Rev. Lett. **77**, 4194 (1996); H.E. Castillo, C.C. Chamon, E. Fradkin, P.M. Goldbart, and C. Mudry, Phys. Rev. B **56**, 10668 (1997).
 - ⁶ David Carpentier and Pierre Le Doussal, Phys. Rev. E **63**, 026110 (2001).
 - ⁷ M.J. Bhaseen, I.I. Kogan, O.A. Soloviev, N. Taniguchi, and A.M. Tsvelik, Nucl. Phys. B **580**, 688 (2000).
 - ⁸ M.R. Zirnbauer, hep-th/9905054 (unpublished).
 - ⁹ M. Janssen, M. Metzler and M.R. Zirnbauer, Phys. Rev. B **59**, 15836 (1999).
 - ¹⁰ Ashvin Chhabra and Roderick V. Jensen, Phys. Rev. Lett. **62**, 1327 (1989).
 - ¹¹ P.W. Anderson, Phys. Rev. **109**, 1492 (1958).
 - ¹² L.S. Levitov, Europhys. Lett. **9**, 83 (1989); Phys. Rev. Lett. **64**, 547 (1990).
 - ¹³ L.S. Levitov, Ann. Phys. (Leipzig) **8**, 697 (1999).
 - ¹⁴ E. Cuevas, Phys. Rev. Lett. **83**, 140 (1999); E. Cuevas, E. Louis, and J.A. Vergés, *ibid.* **77**, 1970 (1996).
 - ¹⁵ A.D. Mirlin, Phys. Rep. **326**, 259 (2000); F. Evers and A.D. Mirlin, Phys. Rev. Lett. **84**, 3690 (2000).
 - ¹⁶ A.D. Mirlin and F. Evers, Phys. Rev. B **62**, 7920 (2000).
 - ¹⁷ E. Cuevas, V. Gasparian and M. Ortuño, Phys. Rev. Lett. **87**, 056601 (2001); E. Cuevas, Phys. Rev. B **66**, 233103 (2002).
 - ¹⁸ E. Cuevas, M. Ortuño, V. Gasparian, and A. Pérez-Garrido, Phys. Rev. Lett. **88**, 016401 (2002).
 - ¹⁹ I. Varga and D. Braun, Phys. Rev. B **61**, R11859 (2000); Imre Varga, *ibid.* **66**, 094201 (2002).
 - ²⁰ V.E. Kravtsov and K.A. Muttalib, Phys. Rev. Lett. **79**, 1913 (1997).
 - ²¹ A.D. Mirlin, Y.V. Fyodorov, F.M. Dittes, J. Quezada, and T.H. Seligman, Phys. Rev. E **54**, 3221 (1996).
 - ²² V.E. Kravtsov and A.M. Tsvelik, Phys. Rev. B **62**, 9888 (2000).
 - ²³ F. Evers, A. Mildenberger, and A.D. Mirlin, Phys. Rev. B **64**, 241303(R) (2001).
 - ²⁴ H. Potempa and L. Schweitzer, Phys. Rev. B **65**, 201105(R) (2002).
 - ²⁵ D. A. Parshin and H. R. Schober, Phys. Rev. B **57**, 10232 (1998).